The official journal of
INTERNATIONAL FEDERATION OF PIGMENT CELL SOCIETIES · SOCIETY FOR MELANOMA RESEARCH
PIGMENT CELL & MELANOMA Research

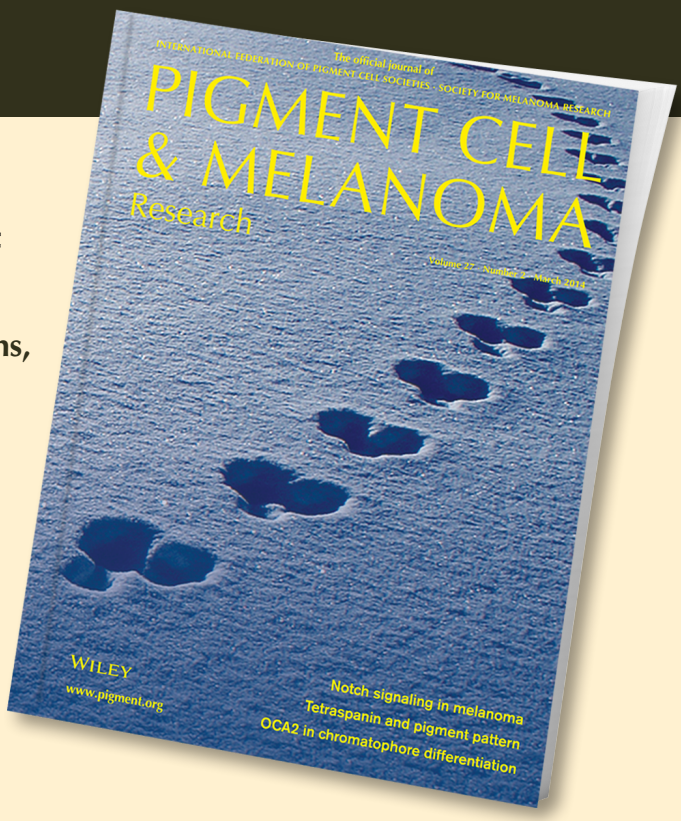

Identification of PLX4032-resistance mechanisms and implications for novel RAF inhibitors

Jaehyuk Choi, Sean F. Landrette, Tiffany Wang, Perry Evans, Antonella Bacchiocchi, Robert Bjornson, Elaine Cheng, Amy L. Stiegler, Symon Gathiaka, Orlando Acevedo, Titus J. Boggon, Michael Krauthammer, Ruth Halaban and Tian Xu

DOI: 10.1111/pcmr.12197
Volume 27, Issue 2, Pages 253–262

Identification of PLX4032-resistance mechanisms and implications for novel RAF inhibitors

Jaehyuk Choi[1,*], Sean F. Landrette[2,*], Tiffany Wang[1], Perry Evans[3], Antonella Bacchiocchi[1], Robert Bjornson[4], Elaine Cheng[1], Amy L. Stiegler[5], Symon Gathiaka[6], Orlando Acevedo[6], Titus J. Boggon[5], Michael Krauthammer[3], Ruth Halaban[1] and Tian Xu[2,7]

1 Department of Dermatology, Yale University School of Medicine, New Haven, CT, USA **2** Department of Genetics, Yale University School of Medicine, New Haven, CT, USA **3** Department of Pathology, Yale University School of Medicine, New Haven, CT, USA **4** Department of Computer Science, Yale University, New Haven, CT, USA **5** Department of Pharmacology, Yale University School of Medicine, New Haven, CT, USA **6** Department of Chemistry and Biochemistry, Auburn University, Auburn, AL, USA **7** Howard Hughes Medical Institute, New Haven, CT, USA

CORRESPONDENCE Jaehyuk Choi and Tian Xu, e-mails: jaehyuk.choi@yale.edu and tian.xu@yale.edu

*Contributed equally to the manuscript.

KEYWORDS BRAF/drug resistance/melanoma/PLX4032/paradox blockers

PUBLICATION DATA Received 16 October 2013, revised and accepted for publication 26 November 2013, published online 27 November 2013

doi: 10.1111/pcmr.12197

Summary

BRAF inhibitors improve melanoma patient survival, but resistance invariably develops. Here we report the discovery of a novel *BRAF* mutation that confers resistance to PLX4032 employing whole-exome sequencing of drug-resistant $BRAF^{V600K}$ melanoma cells. We further describe a new screening approach, a genome-wide *piggyBac* mutagenesis screen that revealed clinically relevant aberrations (N-terminal *BRAF* truncations and *CRAF* overexpression). The novel *BRAF* mutation, a Leu505 to His substitution ($BRAF^{L505H}$), is the first resistance-conferring second-site mutation identified in *BRAF* mutant cells. The mutation replaces a small nonpolar amino acid at the BRAF-PLX4032 interface with a larger polar residue. Moreover, we show that $BRAF^{L505H}$, found in human prostate cancer, is itself a MAPK-activating, PLX4032-resistant oncogenic mutation. Lastly, we demonstrate that the PLX4032-resistant melanoma cells are sensitive to novel, next-generation BRAF inhibitors, especially the 'paradox-blocker' PLX8394, supporting its use in clinical trials for treatment of melanoma patients with BRAF-mutations.

Introduction

Small molecule inhibitors targeted against 'druggable' oncogenic mutations are remarkably effective in the treatment of metastatic cancer. Unfortunately, their efficacy is often limited by the emergence of resistance (Janne et al., 2009). One important obstacle to single-agent therapies is the presence of vast genetic heterogeneity within a tumor and between metastases (Vogelstein et al., 2013). Sequencing analysis has shown that the genomic architecture of cancer cells can vary widely depending on the location of the cells within large tumors (Navin et al., 2011). The clinical significance of this heterogeneity has been demonstrated for colorectal and lung cancers where pre-existing clones with mutations conferred drug resistance (Diaz et al., 2012; Turke et al., 2010).

Significance

Although type I BRAF inhibitors improve overall survival in metastatic melanoma, resistance invariably develops, posing an important obstacle to patient care. Utilizing whole-exome sequencing and a novel forward genetic screening method, we identified a novel $BRAF^{L505H}$ mutation in $BRAF^{V600K}$ melanoma cells, N-terminal *BRAF* truncations, and *CRAF* overexpression, as mechanisms for PLX4032-resistance. The $BRAF^{L505H}$ mutation was present in untreated patient-derived melanoma cells, providing the first genetic evidence in melanoma that pre-existing genetic heterogeneity contributes to 'acquired' resistance. Furthermore, we find that next-generation BRAF inhibitors are effective against PLX4032-resistant cells.

Type I ATP-competitive BRAF inhibitors, such as vemurafenib (PLX4032), are clinically effective for melanomas with oncogenic mutations in *BRAF*, but limited by the rapid emergence of drug resistance (Sosman et al., 2012). Systematic characterization of resistance to these agents is required for the development of effective next-generation therapeutic strategies. Resistance mechanisms identified to date include the overexpression of PDGFR-β (Nazarian et al., 2010), ERBB3 (Abel et al., 2013), or other receptor tyrosine kinases (Girotti et al., 2013), increased anti-apoptotic signaling (Haq et al., 2013), reactivation of MAPK signaling pathway (Maertens et al., 2013; Montagut et al., 2008; Nazarian et al., 2010; Poulikakos et al., 2011; Shi et al., 2012; Whittaker et al., 2013), loss of PTEN (Paraiso et al., 2011), or provision of growth factors from surrounding stromal cells (Straussman et al., 2012; Wilson et al., 2012), reviewed in (Hartsough et al., 2013). Although amplification, gene fusions, and splice variants of the *BRAF* gene have been identified in patients who developed resistance (Botton et al., 2013; Poulikakos et al., 2011; Shi et al., 2012), secondary mutations in the *BRAF* gene have yet to be discovered in patients.

Here, we report the development of a two-armed strategy to identify multiple mechanisms of PLX4032 resistance in melanoma. We developed and validated a versatile genome-wide forward genetic screening strategy that enables the rapid identification of clinically relevant drug resistance mechanisms in cancer cells. The *piggyBac* transposon insertional mutagenesis screen independently verified N-terminal truncations of BRAF and full-length overexpression of CRAF as mechanisms of drug resistance to PLX4032.

More importantly, whole-exome sequencing of unmutagenized PLX4032-resistant $BRAF^{V600K}$ melanoma cells (YUMAC), revealed the first spontaneously occurring second-site mutation in *BRAF* that confers resistance to PLX4032, $BRAF^{L505H}$. We further show that the $BRAF^{L505H}$ mutation precedes exposure to the drug. It is present in a subclone that constitutes 1% of the untreated YUMAC melanoma cells. In addition, we demonstrate that $BRAF^{L505H}$, which was previously identified in human prostate cancer without a concomitant V600 mutation, is itself a MAPK activating oncogenic mutation intrinsically resistant to PLX4032. Finally, we show that next-generation, BRAF inhibitors "paradox blockers", in particular PLX8394, are highly efficient at inhibiting the proliferation of this panel of BRAF-mutant resistant melanoma cells.

Results

piggyBac insertional mutagenesis

We employed a two-armed strategy to identify mechanisms of resistance to PLX4032: (i) a transposon-based mutagenesis screen, and (ii) recovering pre-existing resistant cells from tumor heterogeneity by a rapid clonogenic assay (Figure S1). For this screen, we used YUMAC cells, a patient-derived short-term human melanoma cell culture that harbors a $BRAF^{V600K}$ mutation and is sensitive to PLX4032 (IC_{50} = 0.06 μM) (Halaban et al., 2010).

We developed a conditional *piggyBac* insertional mutagenesis system for mammalian cells in culture and utilized it to conduct a genome-wide genetic screen for PLX4032-resistance. The mutagenic *piggyBac* transposon (*PB[Mut-tetO-KAT]*) up-regulates the expression of endogenous gene products or truncated products upon insertion into the genome in a doxycycline-dependent manner (Figure 1A, B, Figure S1 and Data S1). Using *PB [Mut-tetO-KAT],* we mutagenized five million YUMAC cells harboring, on average, 10 unique transposon insertions. Transposon insertional mutagenized YUMAC cells (YUMAC-TIM) were cultured continuously in medium supplemented with 1.5 μM PLX4032. We isolated 150 resistant clones (TIM-R), which were macroscopically visible after approximately 17 days (Methods). The TIM-R clones were transduced with TetR-KRAB to confirm that the drug resistance is transposon-dependent. Indeed, drug resistance required doxycycline for 130 of the 150 clones (Figure 1C), confirming that PLX4032 resistance was transposon-dependent for the majority of TIM-R.

Linker-mediated PCR coupled to Illumina sequencing was utilized to identify the transposon insertion sites in the first sixteen clones identified (Ni et al., 2013). In this group, only two genes (*BRAF* and *CRAF*) were identified with more than one transposon insertion site in the same orientation (Table S1). Ten of the sixteen TIM-R clones contained an insertion in *BRAF* (TIM-BRAF), and six harbored an insertion in *CRAF* (TIM-CRAF) (Figure 1D). None of the clones had insertions in both *BRAF* and *CRAF*. Consistent with the direction and location of *PB [Mut-tetO-KAT]* insertion, TIM-BRAF expressed an N-terminal truncated BRAF (ΔN-BRAF) (Figure 1, E and F). Similar to the recently identified *BRAF* splice variants ($p61^{BRAF}$) (Poulikakos et al., 2011), these ΔN-BRAF moieties selectively lose the N-terminal RAS-binding domains, which are found in exons 4 through 6. The transposon, in contrast, has an enhancer effect in TIM-CRAF clones, upregulating the full-length gene transcript (Figure 1E, F). Overexpression of ΔN-BRAF or full-length CRAF in another otherwise PLX4032-sensitive BRAF-mutant melanoma cell line (YUSIK-$BRAF^{V600E}$), was sufficient to confer drug resistance (Figure S2), consistent with recently published reports (Montagut et al., 2008; Poulikakos et al., 2011). All of the remaining 115 TIM-R clones displayed upregulation of either Δ*N-BRAF* or *CRAF* as measured by quantitative PCR (data not shown).

Pre-existing BRAF-V600E/L505H drug-resistant YUMAC cells

We examined in parallel whether unmanipulated YUMAC cells harbor pre-existing mutations that confer resistance

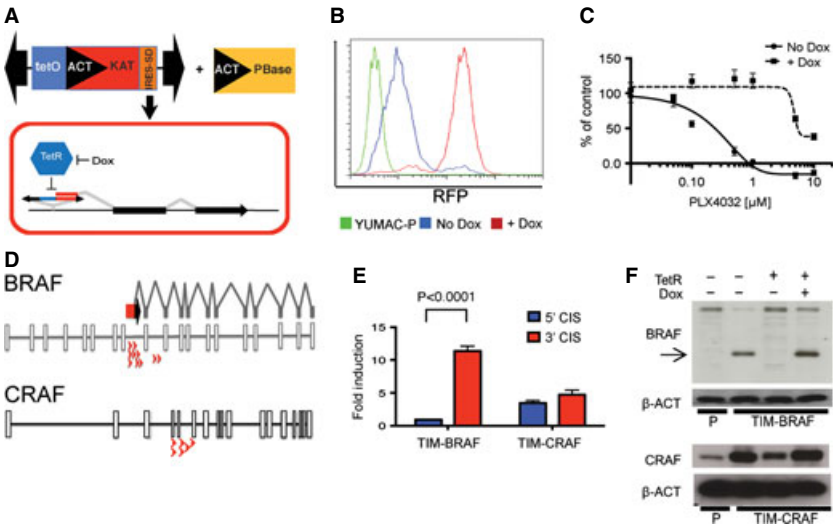

Figure 1. *PB* mutagenesis of YUMAC cell induces PLX4032 resistance. (A) Schematic of *PB[Mut-tetO-KAT]*. The *Actin* promoter (black pointed box) and Katushka red fluorescent protein (red box) couples KAT expression with ectopic expression of a downstream gene or partial gene transcript via the IRES (orange box). The tetO (blue box) allows binding of TetR-KRAB (TetR), which binds and represses expression in the absence of doxycycline (Dox). (B) FACS plots of KAT red fluorescence signal comparing the parental YUMAC cell line (YUMAC-P, green) to YUMAC-TIM cells transduced with TetR-KRAB (TIM-TetR) with (red) and without doxycycline (blue). (C) Dose–response curve of PLX4032 on TIM-TetR in the presence or absence of doxycycline. Cell numbers in increasing concentrations of PLX4032 were determined by CellTiter-Glo assays (72 h). (D) Transposon insertions cluster (red arrowheads) in introns eight and nine of *BRAF* and in introns five and six and exon six of CRAF. (E) Relative expression of *BRAF* and *CRAF* transcripts 5′ and 3′ to the transposon insertion sites in TIM-BRAF and TIM-CRAF clones. Transcript levels were normalized to YUMAC-P. (F) Western blot analysis of BRAF (top) and CRAF (bottom) in YUMAC-TIM. BRAF levels were assessed with an antibody targeting a C-terminal epitope. Protein levels were assessed in YUMAC-TIM and TIM-TetR in the presence or absence of doxycycline.

to PLX4032. Culturing the parental YUMAC cells (YUMAC-P) continuously in PLX4032 revealed that approximately 1% of the cells formed resistant colonies. Whole exome sequencing of six YUMAC-resistant clones and unmutagenized and untreated YUMAC parental cells revealed that all six resistant clones carry a novel dinucleotide mutation (GA>AT) in *BRAF*, which causes an L505H amino acid substitution (Figure 2A, compare YUMAC-P to YUMAC-L505H). This mutation was recently identified by a saturating mutagenesis approach to identify *BRAF* mutations that confer resistance to PLX4032 (Wagenaar et al., 2013).

In addition, we found that there was no change in the *BRAF* copy number. All YUMAC cells have 5 copies of $BRAF^{V600K}$ but no copies of wild-type *BRAF* (Figure 2B), consistent with a previous report (Halaban et al., 2010). The prevalence of the L505H mutation in all six PLX4032-resistant clones was approximately 20%, indicating that the mutation occurs in only one of the five copies of the $BRAF^{V600K}$ gene ($BRAF^{V600K/L505H}$) (Figure 2C, Table S2). The six YUMAC-$BRAF^{L505H}$ clones are derived from the same subclone as they all share the same 12 SNV's, which are not present in the parental PLX4032-sensitive YUMAC cells (Figure S3, Tables S3–5). These data suggested that the L505H substitution in BRAF existed prior to PLX4032 selection. To verify this, we performed deep sequencing of this region in untreated, unmutagenized YUMAC cells, and found that 0.2% of the *BRAF* genes harbor the L505H mutation (Figure 2D). As YUMAC cells carry five copies of $BRAF^{V600K}$, the data suggest that 1% of untreated, unmutagenized YUMAC carry $BRAF^{V600K/L505H}$ (Figure 2E, F).

YUMAC-$BRAF^{L505H}$ clones, like TIM-BRAF and TIM-CRAF melanoma cells, exhibit persistent MEK and ERK activation in the presence of increasing concentrations of PLX4032 (Figure 3A, B). To confirm that the L505H mutation in *BRAF* confers drug resistance, we transduced YUMAC-P with a retroviral vector encoding $BRAF^{V600E/L505H}$, employing vector and $BRAF^{V600E}$ as controls. We performed similar experiments with a retroviral vector encoding $BRAF^{V600K/L505H}$ in another PLX4032-sensitive melanoma cell line, YUGEN8-$BRAF^{V600E/WT}$. The results show that only BRAF carrying the L505H amino acid substitution significantly increased resistance to PLX4032 [IC_{50} from 0.18 to 4.58 μM for YUMAC (P-value < 0.0001) and 0.1 to 1.0 μM for YUGEN8 (P-value < 0.0001)] and activated the MAPK cascade (Figure 3C–E, Figure S4). As expected, the mutation had no effect on sensitivity to MEK1/2 inhibitors or to the treatment with combined MEK-BRAF inhibitors (Figure 3F).

Structural mapping of BRAF L505H

Structural mapping of BRAF residue L505 shows that this residue is located in the C-helix of the kinase domain N-terminal lobe (Figure 4A). It points inward towards the

kinase catalytic cleft. In the co-crystal structure of the BRAF^{V600E} kinase domain with PLX4032 (Bollag et al., 2010), the inhibitor binds proximal to the L505 side chain and van der Waals contacts are made between the L505 side-chain and the propane-1-sulfonamide moiety of the inhibitor (Figure 4A). The presence of the larger polar amino acid at the contact site is therefore predicted to disrupt the binding of PLX4032. A molecular dynamics simulation supports a direct effect of L505H on the binding of PLX4032. The distance between the carbon atom bisecting the two nitrogens in the side-chain of the His505 residue and the sulfur atom in PLX4032 was monitored over the 100 ns simulation (Figure S5). At the end of the simulation, inspection of the active sites indicated that the bound inhibitor moved further away from the A-loop containing the 505th residue in the *BRAF*$^{V600E/L505H}$ mutants compared to *BRAF*^{V600E}. In contrast, docking calculations suggested that there was no deleterious effect of the L505H mutation on the binding of a structurally unrelated type II BRAF inhibitor, such as sorafenib. The binding energy of sorafenib, in fact, slightly improved from −10.5 kcal for binding to *BRAF*^{V600E} and −10.9 kcal for binding to *BRAF*$^{V600E/L505H}$. Consistent with this model, YUMAC-P and YUMAC-

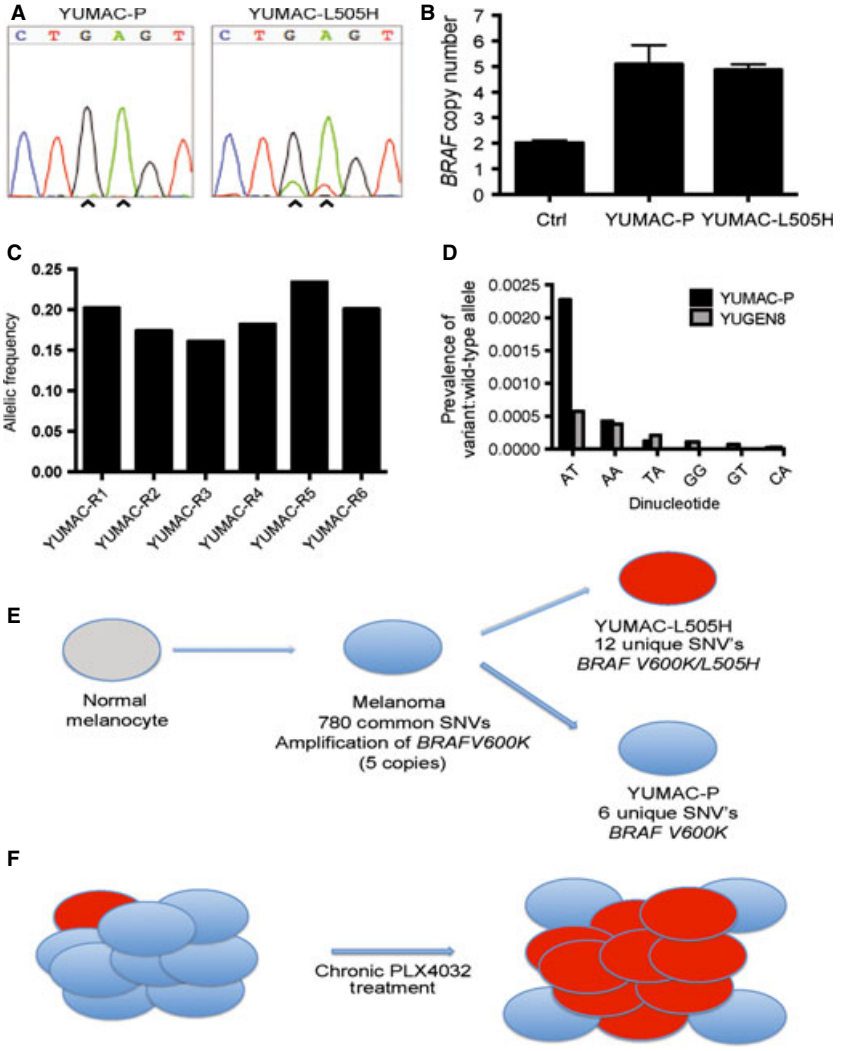

Figure 2. *BRAF*^{L505H} mutation is present in unmanipulated YUMAC PLX4032-resistant clones and at low prevalence in the parental unselected cells. (A) Chromatograph demonstrating AT dinucleotide change in *BRAF* in resistant cells (YUMAC-L505H, black arrows). (B) *BRAF* copy number as determined by quantitative PCR and normalized to multicopy reference control (Qiagen). (C) *BRAF*$^{V600K/L505H}$ allele frequency in the six YUMAC PLX4032 resistant clones calculated from analysis of exome sequencing. The six clones are annotated as YUMAC-R1-R6. (D) The prevalence of dinucleotide substitution at chr 7: 140477793–140477794 (hg19) is plotted from deep sequencing of an 82 bp amplicon utilizing genomic DNA from the YUMAC-P and YUGEN8 cell lines. (E) Proposed model of YUMAC-BRAF^{L505H} evolution. Based on common SNV's, YUMAC- BRAF^{L505H} and YUMAC-P share a common progenitor that has 780 novel SNV's not found in publically available databases. YUMAC- BRAF^{L505H} and YUMAC-P then diverge. YUMAC-BRAF^{L505H} and YUMAC-P have 12 and 6 unique SNV's, respectively. (F) Proposed model for the persistent emergence of YUMAC- BRAF^{L505H} (red) from YUMAC-P (blue) after PLX4032 selection.

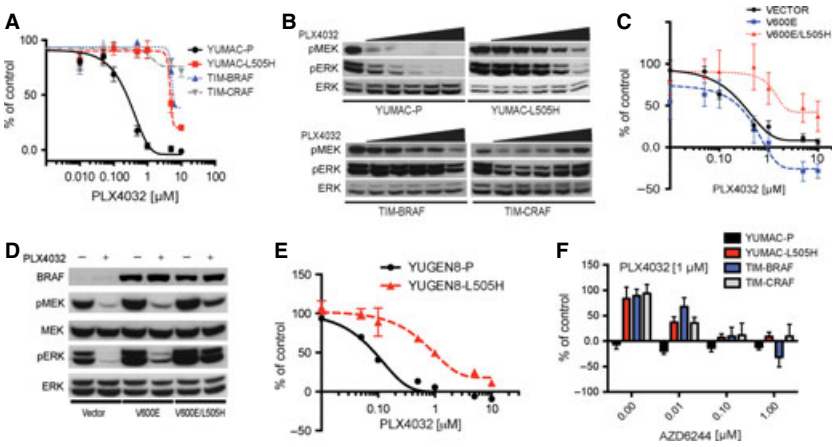

Figure 3. *BRAF*^{L505H} mutation confers resistance to PLX4032. (A) YUMAC-P, YUMAC- BRAF^{L505H}, TIM-BRAF, and TIM-CRAF growth response to increasing concentration of PLX4032. (B) Changes in pMEK and pERK after 18 h treatment of YUMAC-P, YUMAC- BRAF^{L505H}, TIM-BRAF, and TIM-CRAF with DMSO or PLX4032 (0.1, 0.3, 1, 3, or 10 μM). (C) Growth response of YUMAC cells transduced with the indicated BRAF variant to increasing concentrations of PLX4032. (D) Changes in pMEK and pERK in YUMAC cells transduced with the indicated BRAF variant after 18 h of treatment with DMSO or 3 μM PLX4032. (E) Cell proliferation of parental YUGEN8-BRAF$^{V600E/WT}$ (YUGEN8-P) and *BRAF*$^{V600K/L505H}$ expressing YUGEN8 cells in response to increasing doses of PLX4032. (F) Dose response to combined treatment with MEK inhibitor (AZD6244) and PLX4032. The cells were cultured in 1 μM PLX4032 and indicated doses of AZD6244.

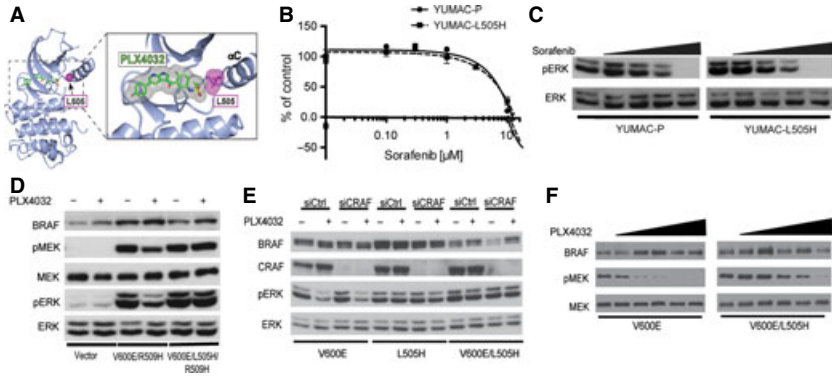

Figure 4. *BRAF*$^{V600K/L505H}$ is intrinsically resistant to PLX4032. (A) Structural model of the BRAF-active site with binding to PLX4032. The amino acid L505 is highlighted in pink and PLX4032 in gray. (B) Growth responses of YUMAC-P and YUMAC-BRAF^{L505H} to increasing doses of sorafenib. (C) Changes in pERK in YUMAC-P and YUMAC-BRAF^{L505H} cells in response to sorafenib. Cells were treated with DMSO or sorafenib (0.1, 0.3, 1, or 3 μM) for 18 h. (D) Changes in pMEK and pERK of 293T cells expressing the indicated BRAF variant after 18 h of treatment with DMSO or PLX4032 (3 μM). **(**E) Down regulation of CRAF does not affect ERK activation in L505H expressing 293T cells. The western blot shows the level of BRAF, CRAF, pERK, and ERK, 72 h after the indicated siRNA transfection followed by 18 h of treatment with DMSO or PLX4032 (3 μM). (F) *BRAF*^{V600E} and *BRAF*$^{V600E/L505H}$ kinase activity in the presence of DMSO or PLX4032 (0.1, 0.3, 1, 3, or 10 μM). The figure shows the total immunoprecipitated BRAF, the phosphorylated levels of the substrate MEK (pMEK), and total MEK.

BRAF^{L505H} are equally sensitive to a type II BRAF inhibitor, sorafenib (Figure 4B, C).

For multiple PLX4032 resistance mechanisms, BRAF dimerization with novel partners drives sustained MAPK signaling in the presence of PLX4032 (Halaban et al., 2010; Poulikakos et al., 2011). Our model, however, predicts that the *BRAF*$^{V600E/L505H}$ kinase is intrinsically resistant to PLX4032. To confirm this, we ectopically expressed BRAF mutants in 293T cells because they do not normally express BRAF-mutant kinases and have minimal baseline MAPK signaling. As our model predicts, drug resistance is independent of dimerization with BRAF or CRAF. Mutating the BRAF dimerization motif (R509H) abolishes resistance conferred by N-terminal truncated BRAF moieties (Poulikakos et al., 2011); however, it has no effect on *BRAF*$^{V600E/L505H}$ (Figure 4D). Similarly, knockdown of CRAF by siRNA has no effect on drug resistance (Figure 4E). Lastly, in vitro kinase assays of immunoprecipitated *BRAF*$^{V600E/L505H}$ demonstrate that the double-mutant kinase is intrinsically resistant to PLX4032 (Figure 4F).

Responses to next-generation RAF inhibitors 'paradox-blockers'

We next tested the sensitivity of YUMAC-BRAF$^{V600K/L505H}$, YUGEN8-BRAF$^{V600E/L505H}$, TIM-BRAF, and TIM-CRAF to

Plexxikon's next-generation RAF inhibitors 'paradox blockers', PLX7904 and PLX8394, the latter set to enter clinical trials. Compared to PLX4032, these agents have unique binding sites in the BRAF active site and are superior inhibitors of wild-type CRAF. Accordingly, PLX7904 has recently been shown to overcome PLX4032 resistance in mutant *NRAS* melanoma cells (Le et al., 2013). Our results show that YUMAC-BRAF$^{V600K/L505H}$, YUGEN8-BRAF$^{V600E/L505H}$ and TIM-CRAF are highly sensitive to these drugs with IC_{50}s approaching nM concentrations (Figure 5A, and Figure S6). PLX7904 is less effective and is not sufficient to overcome resistance conferred by ΔN-BRAF (TIM-BRAF) (P-value = 0.0023). However, PLX8394 efficiently overcomes all three mechanisms of drug resistance and inhibits the MAPK pathway in all resistant cells (Figure 5A, B).

The clinical relevance of the *BRAF^{L505H}* mutation is highlighted by its recent identification in human prostate cancer. Whole-exome sequencing identified a tumor with a *BRAF^{L505H}* mutation without a concurrent *BRAF^{V600}* mutation (Barbieri et al., 2012). To assess whether L505H substitution in BRAF is itself an activating mutation, we expressed *BRAF^{L505H}* and appropriate controls in 293T cells. The *BRAF^{L505H}* mutation is sufficient to activate MAPK signaling in cells and in *in vitro* kinase assays, albeit to a lesser extent than the *BRAF^{V600E}* mutation (Figure 6A, B). As expected from our data in melanoma, MAPK activation by *BRAF^{L505H}* is resistant to PLX4032 but sensitive to MEK inhibitors (Figure 6C–E). We then expressed this construct in immortalized prostate cells to assess its oncogenic function. *BRAF^{L505H}* activates pMEK and pERK (Figure 6F) and promotes anchorage-independent growth of prostate cells (Figure 6G, H).

Discussion

We have discovered the first spontaneously occurring second-site mutation in *BRAF* that confers resistance to PLX4032. Unlike other mechanisms of PLX4032 resistance, this mutation directly disrupts PLX4032-kinase binding. *BRAF^{L505H}* replaces a small non-polar amino acid with a larger polar amino acid at the drug binding site. Because of clashing van der waals forces, computational modeling predicts that this missense mutation reduces the affinity of PLX4032 for its drug target. Our experiments support this model as in vitro kinase assays show that immunoprecipitated BRAF$^{V600E/L505H}$ can both activate MAPK and resist inhibition by PLX4032 in cell-free systems.

Although the patient from whom YUMAC cells were derived unfortunately died prior to the advent of BRAF inhibitors, our data support a model whereby this mutation could have induced 'acquired' drug resistance. As the pool of YUMAC cells is sensitive to PLX4032, we predict that the tumors in this patient would initially shrink with vemurafenib treatment. However, we hypothesize that the subclone carrying *BRAF$^{V600K/L505H}$* would have been present in the patient's untreated tumors, as it is present in 1% of the untreated YUMAC cell line. Therefore, we envisage that she would have 'acquired' resistance quickly due to the unfettered selective expansion of this intrinsically drug-resistant subclone.

The clinical importance of this mutation is further highlighted by its discovery in prostate cancer by whole exome sequencing (Barbieri et al., 2012). We are the first to show that *BRAF^{L505H}* without a concomitant V600 mutation is an oncogenic mutation that is sufficient to activate MAPK signaling and transform human prostate cells. We further show that this mutation like *BRAF$^{V600K/L505H}$* is intrinsically resistant to PLX4032. In contrast, other oncogenic BRAF mutations outside of the V600 amino acid position (for example, L597) are sensitive to PLX4032 (Dahlman et al., 2012). Collectively, our data may suggest that oncogenic BRAF mutations should be individually tested for their sensitivity to targeted RAF inhibitors.

Furthermore, we have engineered a dox-inducible *piggyBac* mutagenesis system that enables a facile, multitiered genome-wide forward screening strategy. The dox-dependent mutagenic cassette enables the rapid confirmation of transposon dependent phenotypes in

A

Cells / Inhibitor	PLX4032	PLX7904	PLX8394
YUMAC-TIM-BRAF	4.5	1.5	0.177
YUMAC-TIM-CRAF	9	0.092	0.024
YUMAC-BRAF^{L505H}	3.4	0.389	0.095
YUGEN8	0.092	0.064	0.033
YUGEN8-BRAF^{L505H}	1.0	0.377	0.035

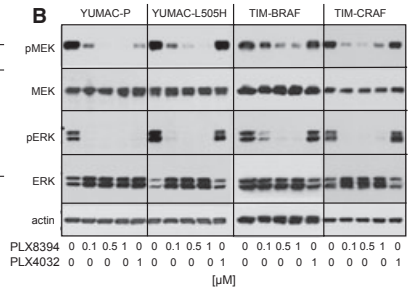

Figure 5. Growth responses of PLX4032-resistant YUMAC cells to 'paradox-blockers'. (A) The table shows the IC_{50} in response to PLX4032, PLX7904, or PLX8394 (see also Figure S5). (B) Changes in pMEK and pERK in response to increasing concentrations of PLX8394, as compared to PLX4032 (1 μM). YUMAC-P, YUMAC-BRAF^{L505H}, TIM-BRAF, and TIM-CRAF were harvested after 4 h exposure to the drugs.

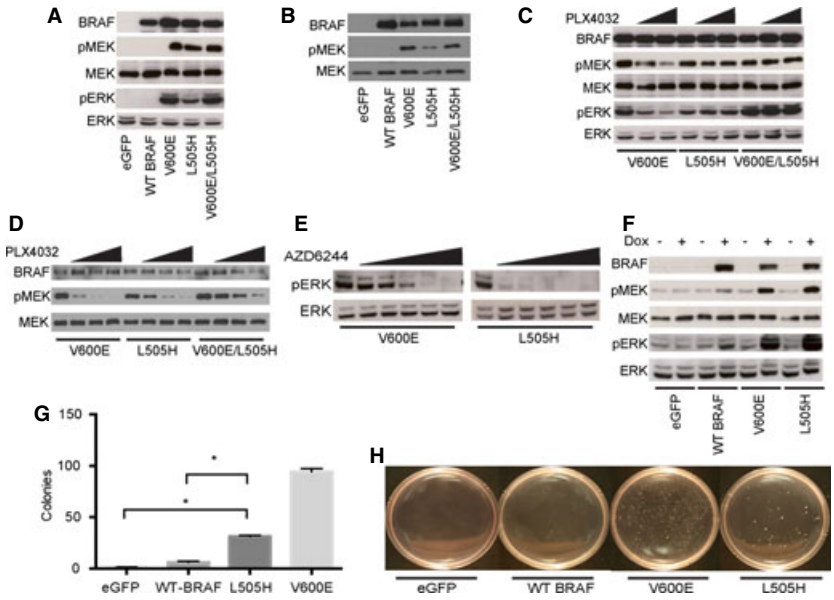

Figure 6. *BRAF^{L505H}* mutation induces oncogenic MAPK signaling. (A) Changes in pMEK and pERK in 293T cells expressing the indicated BRAF variant. (B) In vitro kinase activity of WT (wild-type) *BRAF, BRAF^{V600E}, BRAF^{L505H}, and BRAF$^{V600E/L505H}$*, employing MEK as a substrate. The figure shows the total immunoprecipitated BRAF, the phosphorylated levels of the substrate MEK (pMEK), and total MEK. (C) Changes in pMEK and pERK in 293T cells expressing the indicated BRAF variant (*BRAF^{V600E}*, *BRAF^{L505H}*, or *BRAF$^{V600E/L505H}$*) after 18 h treatment with DMSO or PLX4032 (1 μM, or 3 μM). (D) IP kinase assay performed on lysates from 293T cells expressing the indicated BRAF variant, treated with DMSO, or increasing concentration of PLX4032 (1, 3, or 10 μM) employing MEK as a substrate. (E) Changes in pERK in response to MEK inhibitor (AZD6244). 293T cells expressing the indicated BRAF variant were treated with DMSO, or AZD6244 (0.03, 0.1, 0.3, 1, or 3 μM) for 18 h. (F) Changes in pERK and pMEK in RWPE-1 prostate cells expressing the indicated doxycycline inducible BRAF variant. (G) Soft agar colonies of RWPE-1 prostate cells expressing the indicated doxycycline-inducible BRAF variant; numbers are averages of triplicate cultures after 3 weeks incubation. *indicates a P-value < 0.0001. (H) Representative photographs of RWPE-1 prostate cells colonies in soft agar expressing the indicated BRAF variant after 3 weeks incubation.

clones. Causative insertional gene mutations can then be quickly mapped by next generation sequencing and common-insertion-site analysis. The screen for PLX4032 resistance clearly shows the strengths of this approach, including low cost, quick turnaround, and facile bioinformatics. Furthermore, this approach can easily be adapted to identify mutations and signaling pathways underlying other novel biological processes, including, but not limited to, discovering the resistance mechanisms to other targeted cancer therapies.

Finally, the two-arms of the screen (assaying for drug resistant mutants simultaneously in piggyBac-mutated and unmanipulated YUMAC cells) produced a collection of resistant cell clones that facilitated comprehensive testing of next generation therapeutic strategies. This panel of cell lines encompass the mechanisms of drug resistance employed by the majority of PLX4032-resistant melanomas in patients (reactivation of the MAPK pathway by activating CRAF or reactivating BRAF). We used this panel of cell lines to show that sensitivity to next generation 'paradox-blocker' RAF inhibitors depends on the molecular mechanism of resistance. Overall, however, we found that the pan-RAF inhibitor, PLX8394, is the most potent and broadly effective against all resistance mechanisms, justifying its introduction into clinical trials.

Methods

Cell culture

Patient derived melanoma lines were cultured in OptiMem (Life Technologies, Grand Island, NY, USA) with 5% FBS (Atlanta Biologics, Flowery Branch, GA, USA) and antibiotics (Halaban et al., 2010). The melanoma specimens were collected with participants' informed consent according to Health Insurance Portability and Accountability Act (HIPAA) regulations with a Human Investigative Committee-approved protocol. 293T and RWPE-1 cell lines were obtained from American Type Culture Collection (ATCC) and cultured in DMEM (Life Technologies) with 10% FBS and Keratinocyte Serum Free Media (Life Technologies), respectively. PLX4032, PLX7904, and PLX8394 were kindly provided by Plexxikon, Inc., Berkeley, CA, USA (Gideon Bollag). Sorafenib and AZD6244 were obtained from LC laboratories (Woburn, MA, USA).

Transposon insertional mutagenesis

PB[mut-TetO-KAT] was constructed by modification of *Luc-PB[Mut]* (Landrette et al., 2011). The tetO was obtained from pHUD10-3 (Gossen and Bujard, 1992) and cloned upstream of the CAG promoter. The Katushka red fluorescent protein was amplified from pTurboFP636-C (Evrogen, Moscow, Russia) and cloned 3′ of the ACT promoter. The blasticidin cassette was amplified from pCDNA6 (Invitrogen, Grand Island, NY, USA) and cloned into the NheI site upstream of the tetO. *ACT-PBase* has been previously described (Ding et al., 2005). YUMAC melanoma cells were transfected with *PB[mut-TetO-Kat]* and *ACT-PBASE* at a molar ratio of 1:1 transposon to transposase and selected in 5 μg/ml blasticidin for 7 days.

Expression vectors

TetR-KRAB (Addgene Plasmid 11642) (Szulc et al., 2006), BRAF, $BRAF^{V600E}$ or CRAF cDNAs were cloned into pBabe-puro. L505H, and R509H mutations were introduced by overlapping PCR (Data S1).

Retroviruses were produced by transfection of 10 μg of viral plasmid DNA into the Phoenix-ampho packaging cell line (Swift et al., 2001). Viral supernatants were collected at 48 and 72 h post transfection and used to infect YUMAC cells with 1 μM of polybrene (Millipore, Billerica, MA, USA). Doxycycline inducible 293T and RWPE-1 cell lines were produced with the transposon construct *PBJ[RT]*. *BRAF* cDNAs with a 5′ V5 epitope tag were amplified by PCR and cloned into the AgeI and XbaI sites (Data S1).

Stable cell lines were generated by selection with 2 μg/ml puromycin. Expression was induced with 200 ng/ml doxycycline. For knockdown experiments, CRAF siRNA smartpool (Dharmacon L-003601) or non-targeting control siRNA (Dharmacon D-001810-01) were transfected in 293T cells in 24 wells with DharmaFECT 1 (Dharmacon T-200(01-07)-01) and 72 h later DMSO or PLX4032 was added for 18 h before making cell lysates.

Identifying PLX4032-resistant melanoma cells

Transposon insertional mutagenized YUMAC and unmutagenized YUMAC cells were incubated in medium supplemented with 1.5 μM PLX4032. The medium was replaced every 3 days. Macroscopically visible drug resistant clones were isolated using Pyrex 6x8 mm cloning rings (Corning 3166-6). Clones were than expanded in 1.5 μM PLX4032 for 2 weeks prior to further analysis.

Mapping transposon insertion sites

A linker-mediated PCR protocol, modified for Illumina high-throughput sequencing and mapping (Ni et al., 2013) was utilized to identify the insertion sites.

Real time RT-PCR

RNA was isolated with RNEasy (Qiagen, Valencia, CA, USA). Cell lysates were homogenized by passing through a 20-gauge syringe. Purified RNA was used with a blend of oligo(dT), random primers and iScript reverse transcriptase (Bio-Rad, Hercules, CA, USA) to synthesize cDNA. Real time RT-PCR with SYBR green in the StepOne Real-Time PCR Instrument (Applied Biosystems, Foster City, CA, USA) was performed in triplicate for each sample to determine mRNA levels using the relative standard curve method.

The primers for BRAF transcripts 5′ of the transposon insertion sites are the following:

- F: 5′- AGAGTCTTCCTGCCCAACAA-3′
- R: 5′- TCGGACTGTAACTCCACACCT-3′

The primers for BRAF transcripts 3′ of the transposon insertion sites are the following:

- F: 5′ GCTCCAGCTTGTATCACCATC-3′
- R: 5′- GGATGATTGACTTGGCGTGT-3′

The primers for RAF1 transcripts 5′ of the transposon insertion sites are the following:

- F: 5′- TGCTGTGCAGTGTTCAGACTT-3′
- R: 5′TTGTGTGTTGTGAGGGGGAAC-3′

The primers for RAF1 transcripts 3′ of the transposon insertion sites are the following:

- F: 5′-GGGGGAGCTTCCTTATTCTC-3′
- R: 5′-GCTACCAGCCTCTTCATTGC-3′

To identify the BRAF copy number, we used DNEasy (Qiagen) to isolate genomic DNA from YUMAC-P, 293T, and YUMAC-L505H cells. Real time RT-PCR with SYBR green (Bio-Rad) was performed in the StepOne Real-Time PCR Instrument (Applied Biosystems). The BRAF primers were the following:

- F: 5′-CAGCACCTACACCTCAGCAG-3′
- R: 5′-GGAAAAGAGTAATTCACACAAGCTC

The multicopy reference control was obtained from Qiagen.

Western blot analysis

Cells were incubated with BRAF inhibitors at the indicated concentration, harvested after 4 or 18 h and lysed in ice-cold RIPA lysis buffer with protease and phosphatase inhibitors (Roche, Basel, Switzerland). Total protein was quantified by the BCA Assay (Pierce, Rockford, IL, USA) and 20 μg of protein was used for Western blotting. The antibodies used were phospho-p44/42 MAPK pThr202/Tyr204, (ERK1/2) (Cell Signaling, 4337; Danvers, MA, USA), p44/42 MAPK (ERK1/2) (Cell Signaling, 4695), Phospho-MEK1/2 pSer217/221 (Cell Signaling 9154), MEK 1/2 (Cell Signaling 4694), RAF-1 (CRAF) (Santa Cruz Biotech, sc-227; Santa Cruz, CA, USA), BRAF (Santa Cruz Biotech, sc-166), or β-actin (Sigma, A5441; St. Louis, MO, USA).

Immunoprecipitation (IP) kinase assay

Cells were lysed in ice-cold Kinase Lysis Buffer (50 mM Tris, pH7.5, 1% NP40, 150 mM NaCl, 10% glycerol, 1 mM EDTA) with protease and phosphatase inhibitors (Roche) and lysates were recovered by centrifugation. Lysates were precleared with 25 μl of washed protein A/G agarose (Pierce) and then total protein was quantified by the BCA Assay (Pierce). Lysates (500 μg/each) were incubated with 0.5 μl of anti-V5 (Life Technologies R960-25) and 25 μl of washed protein A/G agarose for 3 h to immunoprecipitate the indicated *BRAF* gene product. After three washes in IP Kinase Lysis Buffer and then one wash with kinase buffer (25 mM Tris, pH 7.5, 10 mM $MgCl_2$), the BRAF kinase assay kit (Millipore 17-359) was used to measure kinase activity by western blotting of phospho-MEK1 according to the manufacturer's instructions.

Proliferation assays

Cell proliferation was measured in 96-wells plate after 3-days incubation with increasing concentrations of drugs (triplicate wells/each) employing the CellTiter-Glo luminescent cell viability assay (Promega, Madison, WI, USA). The IC_{50} values (the dose that elicits 50% inhibition compared to vehicle control) were calculated from the slope of the drug response by linear interpolation. P-values were assessed using two-way ANOVA.

Exome-capture, high-throughput sequencing and sequence validation

The DNeasy purification kit (Qiagen) was used to extract genomic DNA from cell pellets. Whole exomes were enriched from genomic DNA by the Roche/NimbleGen solution-based SeqCap EZ Exome Library capture method following the manufacturer's protocols at the Yale Center for Genome Analysis. The exome-capture area comprised 26.2 Mb. Sequencing was performed with the Illumina HiSeq 2000 as 75-bp paired-end reads following the manufacturer's protocols. The mean coverage depth was 212X. See Data S1 for data analysis. *BRAF* mutations were validated by Sanger sequencing.

Ultra-deep sequencing

We designed PCR primers that flank very short regions (<45 bp) around codon 505 of BRAF.

- F: 5′-CAGCACCTACACCTCAGCAG-3′,
- R: 5′-GGAAAAGAGTAATTCACACAAGCTC-3′

An 82 bp amplicon was generated by PCR utilizing Kapa HiSeq. Illumina TruSeq sequencing adaptors with different indices were ligated to the PCR amplicons and purified using PCR purification kit (Qiagen). All samples were loaded onto a single lane of an Illumina HiSeq 2000 flow cell and subjected to 75 bp paired-end sequencing. A modified version of OPAL (Overlapped Paired-End Alignment) (Narayan et al., 2012) was utilized to correct for sequencing errors and to quantify low-frequency dinucelotides as previously described.

Soft agar assay

RWPE-1 cells were seeded in 60 mm plates at 10^5 cells per plate in 0.4% SeaPlaque agarose in Keratinocyte serum free medium (SFM), layered onto 0.8% agarose in Keratinocyte SFM. Soft agar experiments were performed in triplicate. Colonies (≥200 μm diameter) were imaged and quantified after 3 weeks.

Acknowledgements

We thank Dr. Gideon Bollag, Plexxikon, for the BRAF inhibitors PLX4032, PLX7904, and PLX8394. This work was supported by the Yale SPORE in Skin Cancer funded by the National Cancer Institute grant (1 P50 CA121974, R. Halaban, PI). It was also supported by a Department of Defense Prostate Cancer Synergy award (DOD W81XWH-11-1-0437). JC was funded by a Dermatology Foundation Investigative Research Fellowship and Career Development Award. SFL was funded by an American Cancer Society fellowship (PF-08-256-01-GMC) and an Alex's Lemonade Stand Young Investigator Award.

References

Abel, E.V., Basile, K.J., Kugel, C.H. III et al. (2013). Melanoma adapts to RAF/MEK inhibitors through FOXD3-mediated upregulation of ERBB3. J. Clin. Invest. *123*, 2155–2168.

Barbieri, C.E., Baca, S.C., Lawrence, M.S. et al. (2012). Exome sequencing identifies recurrent SPOP, FOXA1 and MED12 mutations in prostate cancer. Nat. Genet. *44*, 685–689.

Bollag, G., Hirth, P., Tsai, J. et al. (2010). Clinical efficacy of a RAF inhibitor needs broad target blockade in BRAF-mutant melanoma. Nature *467*, 596–599.

Botton, T., Yeh, I., Nelson, T. et al. (2013). Recurrent BRAF kinase fusions in melanocytic tumors offer an opportunity for targeted therapy. Pigment Cell Melanoma Res. *26*, 845–851.

Dahlman, K.B., Xia, J., Hutchinson, K., et al. (2012). BRAF(L597) mutations in melanoma are associated with sensitivity to MEK inhibitors. Cancer Discov. *2*, 791–797.

Diaz, L.A. Jr, Williams, R.T., Wu, J. et al. (2012). The molecular evolution of acquired resistance to targeted EGFR blockade in colorectal cancers. Nature *486*, 537–540.

Ding, S., Wu, X., Li, G., Han, M., Zhuang, Y., and Xu, T. (2005). Efficient transposition of the piggyBac (PB) transposon in mammalian cells and mice. Cell *122*, 473–483.

Girotti, M.R., Pedersen, M., Sanchez-Laorden, B. et al. (2013). Inhibiting EGF receptor or SRC family kinase signaling overcomes BRAF inhibitor resistance in melanoma. Cancer Discov. *3*, 158–167.

Gossen, M., and Bujard, H. (1992). Tight control of gene expression in mammalian cells by tetracycline-responsive promoters. Proc. Natl Acad. Sci. USA *89*, 5547–5551.

Halaban, R., Zhang, W., Bacchiocchi, A., Cheng, E., Parisi, F., Ariyan, S., Krauthammer, M., Mccusker, J.P., Kluger, Y., and Sznol, M. (2010). PLX4032, a selective BRAF(V600E) kinase inhibitor, activates the ERK pathway and enhances cell migration and proliferation of BRAF melanoma cells. Pigment Cell Melanoma Res. *23*, 190–200.

Haq, R., Yokoyama, S., Hawryluk, E.B. et al. (2013). BCL2A1 is a lineage-specific antiapoptotic melanoma oncogene that confers resistance to BRAF inhibition. Proc. Natl Acad. Sci. USA *110*, 4321–4326.

Hartsough, E., Shao, Y., and Aplin, A.E. (2013). Resistance to RAF inhibitors revisited. J. Invest. Dermatol. [Epub ahead of print].

Janne, P.A., Gray, N., and Settleman, J. (2009). Factors underlying sensitivity of cancers to small-molecule kinase inhibitors. Nat. Rev. Drug Discov. *8*, 709–723.

Landrette, S.F., Cornett, J.C., Ni, T.K., Bosenberg, M.W., and Xu, T. (2011). piggyBac transposon somatic mutagenesis with an activated reporter and tracker (PB-SMART) for genetic screens in mice. PLoS ONE *6*, e26650.

Le, K., Blomain, E.S., Rodeck, U., and Aplin, A.E. (2013). Selective RAF inhibitor impairs ERK1/2 phosphorylation and growth in mutant NRAS, vemurafenib-resistant melanoma cells. Pigment Cell Melanoma Res. *26*, 509–517.

Maertens, O., Johnson, B., Hollstein, P. et al. (2013). Elucidating Distinct Roles for NF1 in Melanomagenesis. Cancer Discov. *3*, 338–349.

Montagut, C., Sharma, S.V., Shioda, T. et al. (2008). Elevated CRAF as a potential mechanism of acquired resistance to BRAF inhibition in melanoma. Cancer Res. *68*, 4853–4861.

Narayan, A., Carriero, N.J., Gettinger, S.N., Kluytenaar, J., Kozak, K.R., Yock, T.I., Muscato, N.E., Ugarelli, P., Decker, R.H., and Patel, A.A. (2012). Ultrasensitive measurement of hotspot mutations in tumor DNA in blood using error-suppressed multiplexed deep sequencing. Cancer Res. *72*, 3492–3498.

Navin, N., Kendall, J., Troge, J. et al. (2011). Tumour evolution inferred by single-cell sequencing. Nature *472*, 90–94.

Nazarian, R., Shi, H., Wang, Q. et al. (2010). Melanomas acquire resistance to B-RAF(V600E) inhibition by RTK or N-RAS upregulation. Nature *468*, 973–977.

Ni, T.K., Landrette, S.F., Bjornson, R.D., Bosenberg, M.W., and Xu, T. (2013). Low-copy piggyBac transposon mutagenesis in mice identifies genes driving melanoma. Proc. Natl Acad. Sci. USA *110*, E3640–E3649.

Paraiso, K.H., Xiang, Y., Rebecca, V.W. et al. (2011). PTEN loss confers BRAF inhibitor resistance to melanoma cells through the suppression of BIM expression. Cancer Res. *71*, 2750–2760.

Poulikakos, P.I., Persaud, Y., Janakiraman, M. et al. (2011). RAF inhibitor resistance is mediated by dimerization of aberrantly spliced BRAF(V600E). Nature *480*, 387–390.

Shi, H., Moriceau, G., Kong, X. et al. (2012). Melanoma whole-exome sequencing identifies (V600E)B-RAF amplification-mediated acquired B-RAF inhibitor resistance. Nat. Commun. *3*, 724.

Sosman, J.A., Kim, K.B., Schuchter, L. et al. (2012). Survival in BRAF V600-mutant advanced melanoma treated with vemurafenib. New Engl. J. Med. *366*, 707–714.

Straussman, R., Morikawa, T., Shee, K. et al. (2012). Tumour micro-environment elicits innate resistance to RAF inhibitors through HGF secretion. Nature *487*, 500–504.

Swift, S., Lorens, J., Achacoso, P., Nolan, G.P. (2001). Rapid production of retroviruses for efficient gene delivery to mammalian cells using 293T cell-based systems. Curr. Protoc. Immunol. edited by John E. Coligan… [et al.] Chapter 10, Unit 10 17C.

Szulc, J., Wiznerowicz, M., Sauvain, M.O., Trono, D., and Aebischer, P. (2006). A versatile tool for conditional gene expression and knockdown. Nat. Methods *3*, 109–116.

Turke, A.B., Zejnullahu, K., Wu, Y.L. et al. (2010). Preexistence and clonal selection of MET amplification in EGFR mutant NSCLC. Cancer Cell *17*, 77–88.

Vogelstein, B., Papadopoulos, N., Velculescu, V.E., Zhou, S., Diaz, L.A. Jr, and Kinzler, K.W. (2013). Cancer genome landscapes. Science *339*, 1546–1558.

Wagenaar, T.R., Ma, L., Roscoe, B., Park, S.M., Bolon, D.N., and Green, M.R. (2013). Resistance to vemurafenib resulting from a novel mutation in the BRAFV600E kinase domain. Pigment Cell Melanoma Res. [Epub ahead of print].

Whittaker, S.R., Theurillat, J.P., Van Allen, E., Wagle, N., Hsiao, J., Cowley, G.S., Schadendorf, D., Root, D.E., and Garraway, L.A. (2013). A Genome-Scale RNA Interference Screen Implicates NF1 Loss in Resistance to RAF Inhibition. Cancer Discov. *3*, 350–362.

Wilson, T.R., Fridlyand, J., Yan, Y. et al. (2012). Widespread potential for growth-factor-driven resistance to anticancer kinase inhibitors. Nature *487*, 505–509.

Supporting information

Additional Supporting Information may be found in the online version of this article:

Data S1. Materials and methods.

Figure S1. Forward genetic screening strategy to identify mutations that confer resistance to PLX4032.

Figure S2. Expression of truncated $BRAF^{V600E}$ (ΔN-BRAF) or CRAF confers PLX4032 resistance.

Figure S3. Hierarchical clustering of 6 YUMAC-BRAF (L505H) clones (YUMAC-R1- YUMAC-R6) and parental YUMAC (YUMAC-P) based on unique SNVs.

Figure S4. $BRAF^{L505H}$ is sufficient to confer resistance to PLX4032 in YUGEN8-$BRAF^{V600E}$ melanoma cells.

Figure S5. Distance (Å) over 100 ns of molecular dynamics simulations between: (1) the Leu505 (central C atom) and PLX4032 (S atom) in red for the $BRAF^{V600E}$ mutant; and (2) the His505 (C atom bisecting N atoms) and PLX4032 (S atom) of the $BRAF^{V600E/L505H}$ double-mutant in black.

Figure S6. PLX4032-resistant YUMAC cells are variably sensitivity to PLX7904 and PLX8394.

Table S1. Table of Transposon Insertion Sites in TIM-R clones.

Table S2. Table of L505H allele frequencies in YUMAC-L505H clones.

Table S3. Table depicting the 12 SNVs shared by the six YUMAC-L505H clones.

Table S4. Table listing the 6 SNVs in the YUMAC-P and not found in the YUMAC-L505H clones.

Table S5. Table of the 780 SNVs shared by all YUMAC cells.